New Phytologist

The role of *teosinte glume architecture* (*tga1*) in coordinated regulation and evolution of grass glumes and inflorescence axes

Jill C. Preston[1,2], Huai Wang[3], Lisa Kursel[3], John Doebley[3] and Elizabeth A. Kellogg[1]

[1]Department of Biology, University of Missouri – St. Louis, Research 223, One University Boulevard, St. Louis, MO 63121, USA; [2]Department of Ecology and Evolutionary Biology, The University of Kansas, 8009 Haworth Hall, 1200 Sunnyside Avenue, Lawrence, KS 66045, USA; [3]Laboratory of Genetics, University of Wisconsin, Madison, WI 53706, USA

Author for correspondence:
Jill Preston
Tel: +1 785 864 5837
Email: jcpxt8@ku.edu

Received: *29 June 2011*
Accepted: *10 August 2011*

New Phytologist (2012) **193**: 204–215
doi: 10.1111/j.1469-8137.2011.03908.x

Key words: gene expression evolution, glume architecture, grass, inflorescence architecture, *Zea mays*.

Summary

- Hardened floral bracts and modifications to the inflorescence axis of grasses have been hypothesized to protect seeds from predation and/or aid seed dispersal, and have evolved multiple times independently within the family. Previous studies have demonstrated that mutations in the maize (*Zea mays* ssp. *mays*) gene *teosinte glume architecture* (*tga1*) underlie a reduction in hardened structures, yielding free fruits that are easy to harvest. It remains unclear whether the causative mutation(s) occurred in the *cis*-regulatory or protein-coding regions of *tga1*, and whether similar mutations in *TGA1*-like genes can explain variation in the dispersal unit in related grasses.
- To address these questions *TGA1*-like genes were cloned and sequenced from a number of grasses and analyzed phylogenetically in relation to morphology; protein expression was investigated by immunolocalization.
- TGA1-like proteins were expressed throughout the spikelet in the early development of all grasses, and throughout the flower of the grass relative *Joinvillea*. Later in development, expression patterns differed between *Tripsacum dactyloides*, maize and teosinte (*Z. mays* ssp. *parviglumis*).
- These results suggest an ancestral role for *TGA1*-like genes in early spikelet development, but do not support the hypothesis that *TGA1*-like genes have been repeatedly modified to affect glume and inflorescence axis diversification.

Introduction

Flowering plants have evolved a tremendous number of strategies to increase fitness through modification of their inflorescence and floral structures. The grass family has particularly complex inflorescences and structures surrounding the flowers (Cheng *et al.*, 1983; Clifford, 1987; Ikeda *et al.*, 2004). Each flower (floret) is made up of a gynoecium, androecium, modified inner tepals (lodicules), an adaxial bract (palea) and an abaxial bract (lemma). The flowers are then aggregated into short spikes (spikelets), which are subtended by two more bracts (glumes). Although the gynoecium and androecium are very similar in most grasses, the structure of the paleas, lemmas and glumes, and the arrangement of the spikelets in the inflorescence, all vary extensively among the 12 000 species of grasses.

A few grass species have independently evolved an inflorescence structure in which the spikelets are embedded in the inflorescence axis (rachis). In these species, the axis develops so that it surrounds the developing spikelet, forming a cup-like depression (Clayton & Renvoize, 1986; E. A. Kellogg, pers. obs.). One or both glumes then cover the outside of the spikelet, similar to a trap door hinged at the bottom; the glumes spread outwards from the inflorescence axis at anthesis and then close again after pollination. In inflorescences such as this, the glumes are often leathery or hardened.

Inflorescences with embedded spikelets have originated in several of the grass subfamilies, but are particularly common in the tribe Andropogoneae, subfamily Panicoideae (Clayton & Renvoize, 1986; E. A. Kellogg, pers. obs.). In most members of Andropogoneae, the rachis of the inflorescence breaks apart (disarticulates) at the node below each spikelet, such that the dispersal unit includes the spikelet plus its adjacent internode. In species in which the spikelet is embedded in the rachis, and in which the glumes are hardened, the mature fruit is fully enclosed in a case made up of the rachis internode plus the glume(s). This structure has been postulated to protect the reproductive structures from damage and/or to facilitate seed dispersal (Wilkes, 1967), although its selective value has never been tested. Despite the important ecological and economic implications for such structures, little is known about how their development is controlled at the genetic level.

The best-studied species with spikelets embedded in the rachis and covered with hardened glumes is teosinte in the genus *Zea*. In *Zea* (tribe Andropogoneae, subfamily Panicoideae), variation in the *SQUAMOSA PROMOTER BINDING PROTEIN-LIKE* (*SPL*) gene, *teosinte glume architecture* (*tga1*), underlies a major

quantitative trait locus (QTL) for the domestication of maize (*Zea mays* ssp. *mays*) from its progenitor teosinte (*Z. mays* ssp. *parviglumis*) (Dorweiler *et al.*, 1993; Wang *et al.*, 2005). *SPL* genes have a wide variety of developmental roles in angiosperms – including the regulation of vegetative and inflorescence phase change, vegetative and inflorescence branching and fruit development – and are known to target the regulation of *SQUAMOSA/FRUITFULL* (*SQUA/FUL*)-like genes, commonly involved in inflorescence and flower development (Mandel & Yanofsky, 1995; Klein *et al.*, 1996; Manning *et al.*, 2006; Schwarz *et al.*, 2008; Wang *et al.*, 2009; Jiao *et al.*, 2010; Preston & Hileman, 2010).

Phenotypic differences associated with the maize *tga1* QTL determine the ease with which the fruit can be separated from the surrounding inflorescence structures. Female inflorescences (ears) of teosinte have remarkably hard glumes with high levels of silica deposition and a high ratio of small to large cells in the mesophyll at maturity, deeply invaginated rachis internodes and little elongation of the floral branch (rachilla). Conversely, maize ears have glumes with fewer small cells, more lignin and less silica deposition, little invagination of the rachis and greater elongation of the rachilla (Clayton & Renvoize, 1986; Dorweiler & Doebley, 1997). Introgression of the maize allele into a teosinte background results in less internode invagination, such that the fruit is no longer enclosed by the rachis. Conversely, introgression of the teosinte allele into a maize background causes increased internode invagination and thickening of the outer glume (Wang *et al.*, 2005). These differences suggest that *tga1* is important for controlling both the hardness of the glumes and the growth of the inflorescence axis to enclose the fruit.

The *tga1* alleles of teosinte and maize differ by only seven nucleotides (Wang *et al.*, 2005). One of these differences encodes a nonconservative amino acid substitution from lysine to asparagine at position six in the protein, and has been hypothesized to affect protein stability or function. This is supported by the teosinte-like phenotype resulting from ethyl methanesulfonate mutagenesis of maize, causing a nonconservative mutation at a neighboring amino acid (position five) (Wang *et al.*, 2005). The remaining six changes are located in the promoter region, and have been hypothesized to affect gene regulation. In early- to mid-stage female spikelets, *tga1* mRNA transcript levels are equivalent between maize and teosinte (Wang *et al.*, 2005). The gene is expressed in the floret meristem, gynoecium, lodicules, paleas, lemmas and glumes. By contrast, at the same time points, levels of protein accumulation, as measured by western blots, appear to be markedly different between the two subspecies (Wang *et al.*, 2005). Protein levels are significantly higher in both early and mid-stages of ear development in teosinte and in maize lines carrying the teosinte *tga1* allele (Wang *et al.*, 2005).

The available data suggest that changes to TGA1 protein stability, translational efficiency or function are more probable explanations for the maize phenotype than are changes in the regulation of the *tga1* gene (Wang *et al.*, 2005). Thus, the lysine to asparagine amino acid substitution may be one of the causative sites underlying the morphological diversification of the maize inflorescence. This amino acid change hypothesis predicts that patterns of mRNA expression will be similar between teosinte and maize post-pollination (> 22 mm ear or style elongation (silk) stage), the stage at which hardening of the outer glume and invagination of the rachis occur in teosinte (Dorweiler & Doebley, 1997). Furthermore, if changes in TGA1 protein stability or translational efficiency, rather than protein function, underlie phenotypic differences, distinct patterns of protein accumulation can be predicted between the two.

The developmental role of *tga1* must be more complex than just described for the female inflorescences of maize and teosinte. Although the female spikelets of teosinte are embedded in the rachis and have rock-hard glumes, the male (tassel) spikelets are not embedded and the glumes are firm, but leaf-like. Furthermore, the *TGA1*-like sequences of two distantly related grasses, rice (*Oryza sativa*) and wheat (*Triticum aestivum*), share the lysine residue of teosinte at position six (Wang *et al.*, 2005), suggesting that this is the ancestral state for most grasses. If this residue were perfectly correlated with glume and inflorescence phenotype, rice and wheat should have hard glumes and embedded spikelets, like teosinte. However, the glumes of wheat are leaf-like (membranous to coriaceous), the glumes of rice are tiny and flap-like and neither species has spikelets embedded in the inflorescence axis; in this respect, they are similar to most other grasses. These observations suggest that different developmental pathways are responsible for glume and rachis architecture in male and female teosinte inflorescences, and that the role of *TGA1* in glume and rachis architecture may have diverged more than once within the tribe Andropogoneae.

The sister genus of *Zea* is *Tripsacum* (Lukens & Doebley, 2001; Mathews *et al.*, 2002; Bomblies & Doebley, 2005), which is, like *Zea*, monoecious. Female spikelets of *Tripsacum* have thick hardened glumes that are sunken into the equally hard rachis, although neither the glumes nor the rachis is as solid as those of teosinte. Male spikelets of *Tripsacum* have leathery glumes that are somewhat firmer than those of *Zea*, but much more flexible than the glumes of the female spikelets. Other Andropogoneae species with invaginated internodes and thickened glumes include *Rhytachne*, *Coelorachis* and various other genera in the tribe (*sensu* Clayton & Renvoize, 1986; Mathews *et al.*, 2002). Unfortunately, previous phylogenetic analyses have found little support for relationships within Andropogoneae (e.g. Lukens & Doebley, 2001; Mathews *et al.*, 2002), making the evolutionary history of glume hardening and rachis internode invagination difficult to reconstruct.

In this study, we test the hypothesis that *TGA1*-like genes have an ancestral role in spikelet development by assessing the pattern of TGA1 protein expression in the early stages of inflorescence development across representative grass species and a closely related grass outgroup. In addition, to evaluate the role of *TGA1*-like gene evolution in glume thickening and rachis invagination, we generated a phylogeny of *TGA1*-like genes, and compared patterns of amino acid sequence variation and protein expression with inferred shifts in inflorescence morphology. Finally, to distinguish between alternative hypotheses for *tga1* diversification between teosinte and maize, we compared mRNA and protein expression patterns in early- and late-stage inflorescences of both subspecies.

Materials and Methods

Plant material and growth conditions

Seeds of maize W22 and Mo17, *Avena strigosa* (Preston 18), sorghum (*Sorghum bicolor*) (Malcomber 3116), *Eleusine indica* (PI217609), green millet (*Setaria viridis*) (PI204624) and *Tripsacum dactyloides* (Kellogg 4) were obtained from the United States Department of Agriculture (USDA), or collected in the field (*T. dactyloides*), and grown at the University of Missouri – St. Louis or the University of Wisconsin – Madison (USA) (maize Mo17) at 20–22°C under constant light. Seeds of *Streptochaeta angustifolia* (Malcomber 3123) were collected by Lynn G. Clark and grown at the University of Missouri – St. Louis on vermiculite in a humid chamber under constant light. Inflorescence material from teosinte (PI384065, PI384071, Ames21814) was harvested from plants grown at the University of Missouri – Columbia by Sherry Flint-Garcia. Other species included in the phylogenetic and expression analyses were grown from seed stocks at the University of Missouri – St. Louis under standard glasshouse conditions.

Sequencing and phylogenetic analysis

Partial *TGA1*-like, *ndhF*, *phyB* and *waxy* sequences were isolated from genomic DNA of representative Andropogoneae and non-Andropogoneae panicoids, nonpanicoid grasses and the nongrass outgroup *Joinvillea ascendens* (Joinvilleaceae) listed in Supporting Information Tables S1 and S2. Total DNA extractions were performed following Malcomber & Kellogg (2006). *ndhF*, *phyB* and *waxy* genes were amplified as described previously (Mathews *et al.*, 2002). *TGA1*-like genes were amplified using the forward primers 482F (5′-AGTGCAGCAGGTTCCATCTACT-3′), 681F (5′-GATSAAAACCGAGGAGAGYCC-3′) or 1000F (5′-GACTCSGAYTGTGCTCTCTCTC-3′) and the reverse primer 1368R (5′-TACTGCCAYGAGAASGGC-3′). Each primer combination amplified exons two and three, part of exon two and exon three, and part of exon three, respectively. Cycling parameters were 94°C for 5 min, followed by 30 cycles of 94°C for 30 s, 55°C for 30 s and 72°C for 1 min, with a final extension of 72°C for 10 min. PCR fragments were purified and cloned into the pGEM-T easy vector (Promega, Madison, WI, USA). Plasmid DNA was cleaned by alkaline lysis and sequenced using the plasmid primers T7 and SP6. Sequencing reactions were carried out using the BigDye 3.1 terminator cycle sequencing protocol (Applied Biosystems, Foster City, CA, USA), and analyzed on an ABI capillary sequencer (Applied Biosystems). Sequence quality was assessed using phred (Ewing *et al.*, 1998).

Sequences with phred scores above 20 were manually aligned in MacClade 4 (Maddison & Maddison, 2003). Phylogenetic analyses were performed on the *TGA1* nucleotide alignment and a combined alignment of *ndhF*, *waxy*, *phyB*, *tb1* and *TGA1*-like genes using GARLI 0.951 and MrBayes 3.1.2 following model optimization in MrModelTest (Ronquist & Huelsenbeck, 2003; Nylander, 2004; Zwickl, 2006). Maximum likelihood (ML) analyses were run using 10 random addition sequences with 500 bootstrap replicates, implementing the HKY + I + Γ (*TGA1*) or GTR + I + Γ (combined) model of evolution based on the results from MrModelTest 2.2. Bayesian analyses were run twice for ten million generations, sampling every 1000 generations, with 25% of trees discarded as burn-in. Gaps were treated as missing data. Trees were rooted with orthologous sequences from the nongrass outgroup *J. ascendens* (*TGA1*-like) or *Pennisetum alopecuroides* (Paniceae) and *Axonopus fissifolius* (Paniceae) (combined) and supplemented with previously generated sequences from GenBank (Tables S1, S2).

To determine the identity of residue six (the amino acid that varies between teosinte and maize *tga1*), a 460-bp fragment was amplified from maize, teosinte, *Bouteloua gracilis* (K-1976-198) (Chloridoideae) and *Rottboellia aurita* (Panicoideae) using the primers Tga1-position1F (5′-ATGGATTGGGATCTCAA-3′) and Tga1-SBP-Rev (5′-TTGGAGTGCGSCTCGCACACCT-TGT-3′). PCR conditions were as described above. To identify potential SPL protein consensus binding sites, putative promoter and coding regions were obtained from rice (Ehrhartoideae), *Brachypodium distachyon* (Pooideae), sorghum (Panicoideae), *Setaria italica* (Panicoideae) and maize (Panicoideae) genomic sequences corresponding to the duplicated grass *FUL*-like genes (Fig. S1). These sequences were used to search for the core consensus sequence CCGTAC (Birkenbihl *et al.*, 2005; Liang *et al.*, 2008).

Character state reconstructions

Glume hardness and the extent of rachis internode invagination were determined for species available in the herbarium collection of the Missouri Botanical Gardens. Glumes were scored as membranous to coriaceous (0) or hard (1), based on the ease of penetration with a needle, whereas rachis internodes were scored as flat to terete (0) or concave (1), based on their overall shape and invagination. In order to reconstruct character state transitions, the likelihood of each glume and internode state was estimated under the Mk1 (single rate of change between states) model of evolution for each node of the best ML tree by tracing characters over the 312 most likely tree topologies in Mesquite version 2.01 (Maddison & Maddison, 2006, 2007).

Expression analysis

Inflorescences at different stages of development were fixed in FAA (47.5% (v/v) ethanol, 5% (v/v) acetic acid, 3.7% (v/v) formaldehyde (Sigma, St. Louis, MO, USA)) using vacuum infiltration. To increase the definition of the cell walls, tissue was stained with 1% eosin Y in 95% ethanol, and dehydrated into paraffin wax, following Jackson (1991). Ribbons of 8-μm longitudinal sections were cut, mounted on Probe-On-Plus microscope slides (Fisher Scientific, Pittsburg, PA, USA) and left to dry at 37°C overnight.

In situ hybridization was performed as described by Jackson *et al.* (1994) using a 500-bp mRNA probe from the 3′ end of

maize *tga1*. As the sequence of this probe was 96% identical to a closely related maize paralog (see Results), hybridization shows expression of both paralogous genes. Sense and antisense riboprobes were generated using T7 and SP6 Megascript *in vitro* transcription kits (Ambion Inc., Austin, TX, USA) with digoxygenin-labeled UTP (Roche, Indianapolis, IN, USA), according to the manufacturer's instructions. Probe hydrolysis followed Jackson (1991). Probe hybridization, washing, immunolocalization and photography followed Jackson *et al.* (1994) and Malcomber & Kellogg (2004). Immunolocalization was performed following Lucas *et al.* (1995) using the TGA1 antibody described in Wang *et al.* (2005). Photographs were imported into Adobe Photoshop and adjusted for contrast, brightness and color balance.

Allele-specific expression assay

We employed an allele-specific assay of *not1* and *tga1* accumulation in the F_1 hybrids of inbred maize and teosinte lines. Seven teosinte inbreds (TIL1, TIL3, TIL5, TIL9, TIL11, TIL14 and TIL25) were used as pollen parents to two or more maize inbreds (B73, CML103, Ki3, Mo17, Oh43 and W22), creating a total of 27 F_1 hybrids (Tables S3, S4). Total cellular RNA was isolated from 5–10 immature ears from one or two plants of each cross; 5-μg aliquots of each of the RNA samples were DNase treated and reverse transcribed (RT) using a polyT primer and Superscript III reverse transcriptase (Invitrogen, Carlsbad, CA, USA), following the manufacturer's instructions. The integrity of the cDNA was checked using 0.5 μl of the RT reactions as the template for PCRs with the actin primers WH182 (5′-CCAAGGCCAACAGAGAGAAA-3′) and WH183 (5′-CCAAACGGAGAATAGCATGAG-3′). The same actin primers were also used to check for genomic DNA contamination. In all cases, the actin primer check was negative for genomic DNA contamination. The RT reactions were diluted and 1-μl aliquots were employed as the template for PCRs using two sets of fluorescently labeled primers: TNW120F (5′ FAM labeled; 5′-ATCCTGCCCCGCCGTGCAG-3′) and TNW121R (5′-CACGAGAAGGGCATCGACGACGAG-3′) to amplify *not1*, and TNW124F (5′ FAM labeled; 5′-GCGATTCTCACCATTTGCGCATC-3′) and TNW126R (5′-AGGCGTGGCGGCTCCCAG-3′) to amplify *tga1* (TAQ Core Kit, Qiagen, Valencia, CA, USA). PCR products were assayed on an ABI 3700 fragment analyzer and peak areas were determined using Gene Marker version 1.70.

In order to perform the allele-specific expression assay, we utilized the fact that the maize and teosinte parents have different allele sizes for both *not1* and *tga1*. Both pairs of TNW primers flank an indel in the respective gene and amplify different sized products for the maize and teosinte parents. The relative message level associated with the two chromosomes in each sample was calculated as the ratio of the area under teosinte/maize allele peaks. The same assay was also performed with the DNA from each of the plants used for RNA extraction to assess any bias in allele amplification in PCR. This analysis revealed that the ratio of the maize/teosinte allele was on average 1.63 for *not1* and 1.10 for *tga1*, indicating that the teosinte allele was slightly underrepresented in both cases. Measurements for the area of the teosinte alleles were therefore multiplied by the factor determined by DNA from the particular plant, and the final message level ratios were calculated with the corrected teosinte areas.

Results

Phylogenetic analysis and amino acid diversity of *TGA1*-like genes

Homologs of *tga1* were amplified and sequenced from 26 taxa, comprising 25 grasses and one nongrass outgroup (*J. ascendens*, Joinvilleaceae) (Table S1). In genes of all species, the binding site for microRNA156 (*Corngrass1* (*Cg1*)) (Chuck *et al.*, 2007) was fully conserved. ML and Bayesian phylogenetic analyses were largely concordant. Well-supported relationships of *TGA1*-like genes outside the Andropogoneae (ML bootstrap above 70%, posterior probabilities above 95%) largely followed known generic relationships (GPWG, 2001; Sánchez-Ken *et al.*, 2007) (Fig. 1), except that *Orthoclada laxa* (Panicoideae) was sister to PACMAD grasses, although without support; we interpret this as an artifact created by sparse sampling outside Panicoideae. Within Andropogoneae there was little resolution, and internal branches were relatively short (Fig. 1). However, the predicted sister relationship between the genes of maize and teosinte was strongly supported (100% ML bootstrap; 100% posterior probability), and there was moderate to strong support for an Andropogoneae clade excluding *Coix lacryma-jobi* and *S. bicolor* (70% ML bootstrap; 100% posterior probability) (Fig. 1).

In contrast with all other sampled taxa, maize and teosinte *tga1* had a duplicate locus that was found to be located on the same chromosome, *c.* 270 kbp from *tga1*. Given the proximity of this *tga1* duplicate, we have named it *neighbor of tga1* (*not1*). *tga1* (designated GRMZM2G10511) and *not1* (designated AC233751.1_FG002) are located at positions 44 508 235–44 512 898 and 44 779 972–44 784 721, respectively, on chromosome 4 of the maize B73 Reference Genome version 2. Sequencing from the maize inbred line W22 revealed 87% amino acid identity between *tga1* and *not1*, and these fell into two well-supported sister clades, each containing a sequence from maize and teosinte (Fig. 1). Thus, the two *Zea TGA1*-like genes are inferred to have arisen from a duplication event after the divergence of *Zea* and *Tripsacum*, but before the divergence of teosinte from modern maize.

A section of *TGA1*-like genes spanning the start codon and part of the highly conserved SBP domain was amplified from maize (*not1*), teosinte (*not1*), *B. gracilis* and *R. aurita*, and aligned with previously sequenced genes from *O. sativa*, *S. italica*, *S. bicolor*, teosinte (*tga1*) and maize (*tga1*). This region contains the lysine to asparagine change (position six) between *tga1* orthologs of maize and teosinte, and the amino acid (position five) that was mutated in maize by ethyl methanesulfonate mutagenesis, resulting in a teosinte-like phenotype (Wang *et al.*, 2005). In all cases, residue five was a phenylalanine, as in both maize and teosinte *tga1*, and residue six was a lysine, as in teosinte

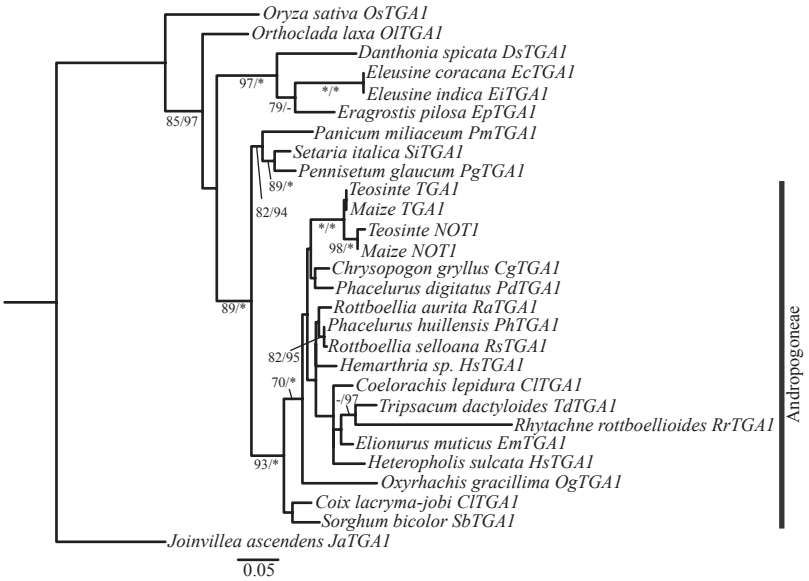

Fig. 1 Maximum likelihood (ML) phylogram showing relationships of grass *TGA1*-like genes. A gene duplication event is inferred to have occurred in the common ancestor of *Zea*, giving rise to the paralogous genes *tga1* and *not1*. The remaining relationships largely track the well-supported species phylogeny (GPWG, 2001). ML bootstrap values > 70% (left) and Bayesian posterior probabilities > 90% (right) are denoted below the branches; 100% support values are indicated with an asterisk. Dashes indicate no support where applicable.

tga1, indicating that this region is highly conserved across Andropogoneae and grasses as a whole.

To determine whether TGA1-like proteins have the potential to regulate spikelet development through the direct regulation of genes known to be involved in spikelet development, *FUL*-like genes from multiple grasses were examined for the SPL protein consensus binding sequence CCGTAC (Birkenbihl *et al.*, 2005; Liang *et al.*, 2008). For every target species, one or more consensus binding sites were found within the putative promoter and/or intronic region of each *FUL1* and *FUL2* gene (Fig. S1). For example, in the rice *FUL1* gene (*OsMADS14*) *sensu* Preston & Kellogg (2006), three binding sites (italic type) were found, one (TT*CCGTAC*GA) 4410 bp upstream of the protein-coding start site and two (CC*CCGTAC*GA and CT*CCGTAC*TT) within the first intron; in the rice *FUL2* gene (*OsMADS15*), three (GA*CCGTAC*GA, GC*CCGTAC*CA and GC*CCGTAC*CA) binding sites were found 394, 3965 and 4028 bp upstream, respectively, of the protein-coding start site. By contrast, a putative SPL binding site was only found for one of the *FUL3* genes examined. The rice *FUL3* gene (*OsMADS18*) had one binding site (CA*CCGTAC*CC) 5232 bp upstream of the protein-coding start site; no consensus binding sites were found within the putative promoter and intronic regions of *S. italica*, *S. bicolor* or *Z. mays* *FUL3* orthologs.

Andropogoneae phylogeny and inflorescence trait evolution

In order to estimate the number and direction of shifts in glume hardening and rachis internode invagination within Andropogoneae, we supplemented previously generated *ndhF*, *waxy*, *phyB* and *tb1* sequences with newly generated *TGA1* sequences, and inferred species relationships (Spangler *et al.*, 1999; Lukens & Doebley, 2001; Mathews *et al.*, 2002) (Table S2; Fig. S2). We found no strongly supported topological differences between trees on the basis of individual markers, and therefore carried out phylogenetic analyses based on combined sequences (Spangler *et al.*, 1999; Lukens & Doebley, 2001; Mathews *et al.*, 2002; this study). The best ML tree based on combined analyses resolved some of the internal relationships within Andropogoneae with high support, including a close relationship between *Coelorachis afraurita*, *Coelorachis selloana*, *Rottboellia* species and *Phacelurus huillensis*, and between *Hemarthria* species and *Heteropholis sulcata* (Fig. S2). Similar to previous analyses based on individual markers, deep branches of the tree were very short and showed little support between groups (Spangler *et al.*, 1999; Lukens & Doebley, 2001; Mathews *et al.*, 2002). For example, the position of *Elionurus muticus* was unstable within the larger *Coelorachis/Zea* clade (Fig. S2; data not shown). This supports the hypothesis of a rapid radiation during the diversification of Andropogoneae subtribes (Celarier, 1956; Spangler *et al.*, 1999).

We used the best ML tree based on the combined dataset to reconstruct the evolution of glume and inflorescence axis traits within Andropogoneae based on ML (Fig. 2). In the case of glume morphology, membranous to coriaceous glumes are inferred as the ancestral state of the Andropogoneae. However, hard glumes are inferred to have evolved between four to seven times independently, followed by four to five independent secondary reductions in glume hardness (Fig. 2). Similar to maize, the secondary reduction of glume hardness in *P. huillensis*, *Urelytrum digitatum* and the *Hemarthria/Heteropholis* clade was strongly supported by both morphological and phylogenetic data; it remains unclear whether coriaceous glumes were secondarily derived in *E. muticus* and *Chionachne koenigii*.

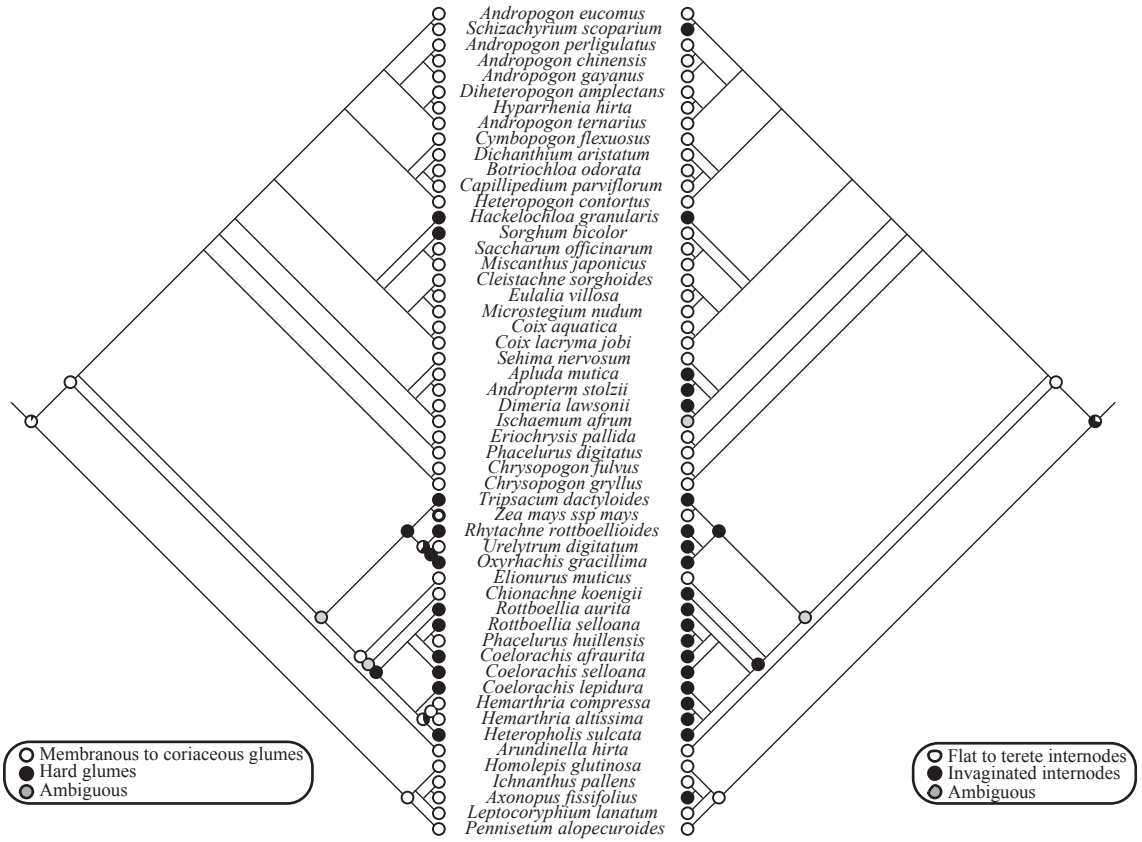

Fig. 2 Glume (left) and rachis internode (right) character state reconstructions within a morphologically variable monophyletic Andropogoneae clade. Character states were reconstructed on the best maximum likelihood (ML) tree from the combined analysis inferred from a variable set of 312 ML trees. Pie charts indicate the proportional likelihood that an ancestor had a particular character state, and are shown only when the probability of a character state is inferred to have changed.

Similar analyses for inflorescence axis morphology reconstructed the ancestor of Andropogoneae as having flat to terete internodes, with four to six transitions to invaginated internodes across the phylogeny (Fig. 2). Morphological data clearly support the independent loss of rachis internode invagination in maize and *E. muticus*. However, topological uncertainty makes it equally likely that flat internodes are ancestral or, instead, evolved secondarily in *E. muticus*.

TGA1-like protein expression

In order to test whether TGA1-like proteins have an ancestral role in spikelet/flower development, and whether changes in their expression correlate with changes in glume hardening and invagination of the inflorescence axis, we compared expression patterns across representative grasses and a closely related outgroup (*J. ascendens*) that vary in inflorescence morphology (Figs 3, 4). Expression patterns were consistent with an ancestral role for *TGA1*-like genes in spikelet development, but did not support the hypothesis that modification of TGA1-like protein expression underlies shifts in glume and rachis internode morphology.

Joinvillea ascendens has conventional monocot flowers comprising outer tepals, inner tepals, stamens and a gynoecium (Preston *et al.*, 2009). Expression of JaTGA1 was evident in all organs of the *J. ascendens* flower, but was absent from the subtending floral bract and branch (Fig. 3a). Unlike *J. ascendens* and other grasses, the early diverging species *S. angustifolia* does not have tepals and lacks true spikelets and glumes. However, previous studies have inferred bracts 1–5 to be transformationally homologous to glumes, and bracts 6–8 to be transformationally homologous to outer tepals and lemmas/paleas (Preston *et al.*, 2009). In early *S. angustifolia* flower development, SaTGA1 was detected in bracts 1–11, but was absent from the inflorescence branch base, presumed to be homologous to a bract subtending the floral unit (Preston *et al.*, 2009) (Fig. 3b). In mid- to late stages of inflorescence development, SaTGA1 was no longer detectable in bracts 1–6, but was strongly expressed in bracts 7–11 and reproductive structures (Fig. 3c).

In grasses with true spikelets, TGA1-like protein was detected in both outer and inner glumes, and within all floret organs at early stages of development, regardless of glume and inflorescence axis morphology (Fig. 3). In the pedicellate spikelets of *A. strigosa*, AsTGA1 was expressed in the membranous glumes, and in all organs of the bisexual proximal florets and reduced distal florets (Fig. 3d). Likewise, in mid-stage development of *E. indica* and *S. viridis* spikelets, EiTGA1 (Fig. 3e) and SvTGA1 (Fig. 3f) were expressed in all floral organs. However, at this stage, very little

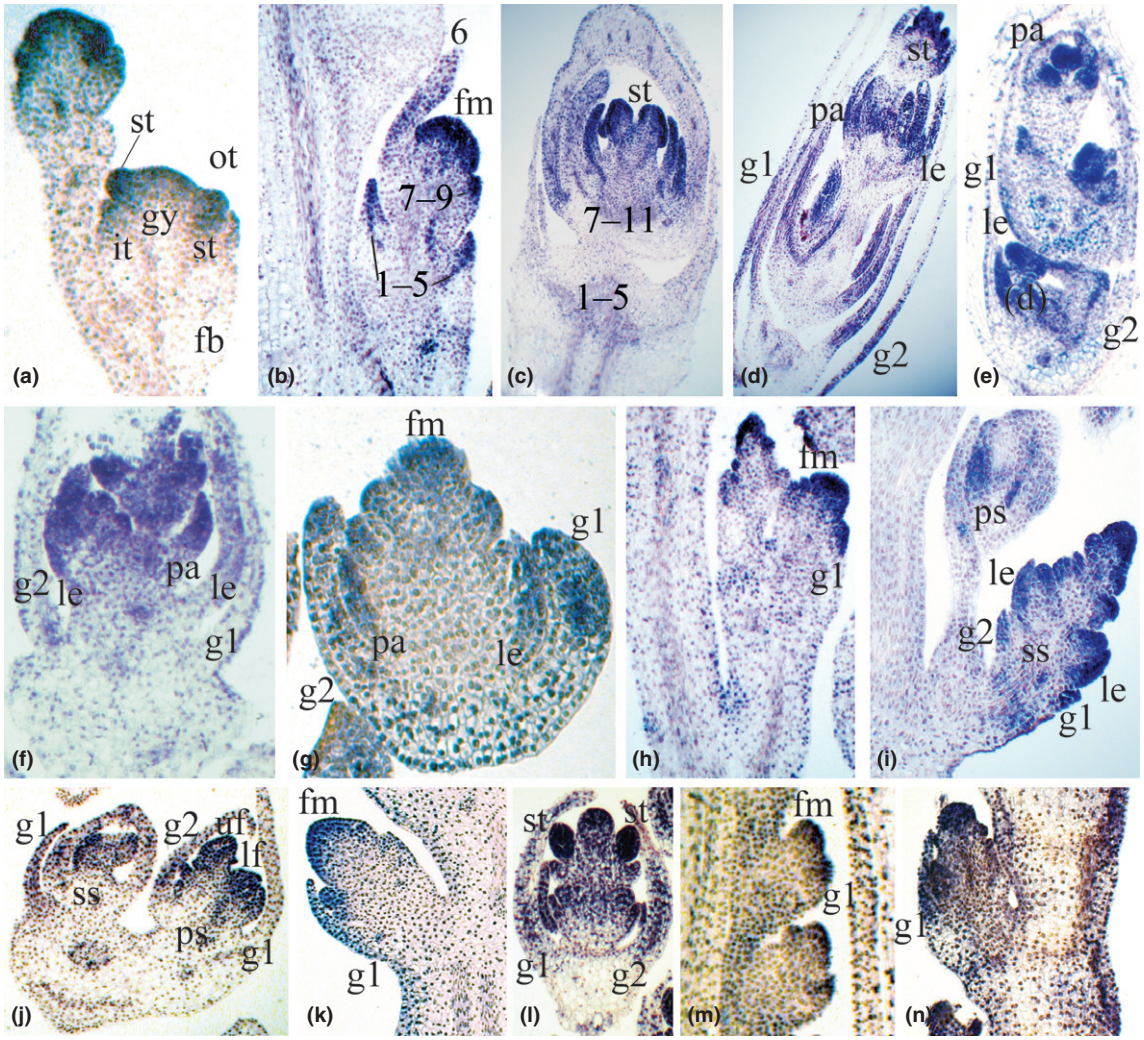

Fig. 3 TGA1-like protein immunolocalization in early- to mid-stage spikelets and flowers of grasses and a grass outgroup. (a) Typical monocot flower of the nongrass outgroup, *Joinvillea ascendens*, with associated floral bracts and branches. JaTGA1 expression is confined to the floral organs. (b, c) Spikelet equivalents of *Streptochaeta angustifolia*; SaTGA1 is expressed in floral bracts 1–9 (numbered) and in the floral meristem during early development (b), and in floral bracts 7–11, stamens and the emerging gynoecium at the mid-stage of development (c). (d) AsTGA1 is expressed in all floret organs and glumes of *Avena strigosa*. (e) EiTGA1 is expressed in all floret organs, but not glumes, during mid-stage *Eleusine indica* spikelet development. (f) SvTGA1 is expressed in all floret organs, but not glumes, during mid-stage *Setaria viridis* spikelet development. (g) Immature spikelet of *Coix lacryma-jobi*; ClTGA1 is detectable in all organs of developing spikelets. (h, i) SbTGA1 is expressed in all organs of both pedicellate and sessile spikelets at early to mid-stages of *Sorghum bicolor* development. (j) TdTGA1 is expressed in all floral organs and glumes of female *Tripsacum dactyloides* spikelet pairs. (k, l) Female (k) and male (l) inflorescences of maize show the same pattern of TGA1/NOT1 expression in all spikelet organs and in the rachis wall. (m, n) Male (m) and female (n) inflorescences of teosinte show the same pattern of TGA1/NOT1 expression as maize. fb, floral bract; fm, floral meristem; g1, outer glume; g2, inner glume; gy, gynoecium; it, inner tepal; le, lemma; ot, outer tepal; pa, palea; ps, pedicellate spikelet; ss, sessile spikelet; st, stamen.

protein was detectable in the membranous subtending glumes of both species.

Within Andropogoneae, all sampled species, with the exception of *S. bicolor*, are monoecious. In *S. bicolor*, SbTGA1 was expressed in all organs of both the bisexual sessile spikelets that have very hard glumes, and the male/sterile pedicellate spikelets that have coriaceous glumes, at early to mid-stages of spikelet development (Fig. 3h,i). In *C. lacryma-jobi*, ClTGA1 was expressed in the coriaceous glumes and floral organs of male and female *C. lacryma-jobi* inflorescences (Fig. 3g). Similarly, TdTGA1 protein was detectable in hard glumes and all floral organs of young *T. dactyloides* female spikelets (Fig. 3j). Finally, cumulative TGA1/NOT1 expression was evident in young to mid-stage glumes, inflorescences axes and all floral organs of both female and male maize (Fig. 3k,l) and teosinte (Fig. 3m,n) spikelets.

In contrast with early- to mid-stage development, late-stage patterns of protein expression differed markedly among *T. dactyloides*, teosinte and maize (Fig. 4). In late-stage spikelet development of *T. dactyloides*, little TdTGA1 protein was detected in the glumes of male (Fig. 4a) or female (Fig. 4b) spikelets, or within maturing floral organs of female spikelets (Fig. 4b); expression was still detectable in late-stage male flowers in the lodicules and stamens (Fig. 4a). Furthermore, at both early

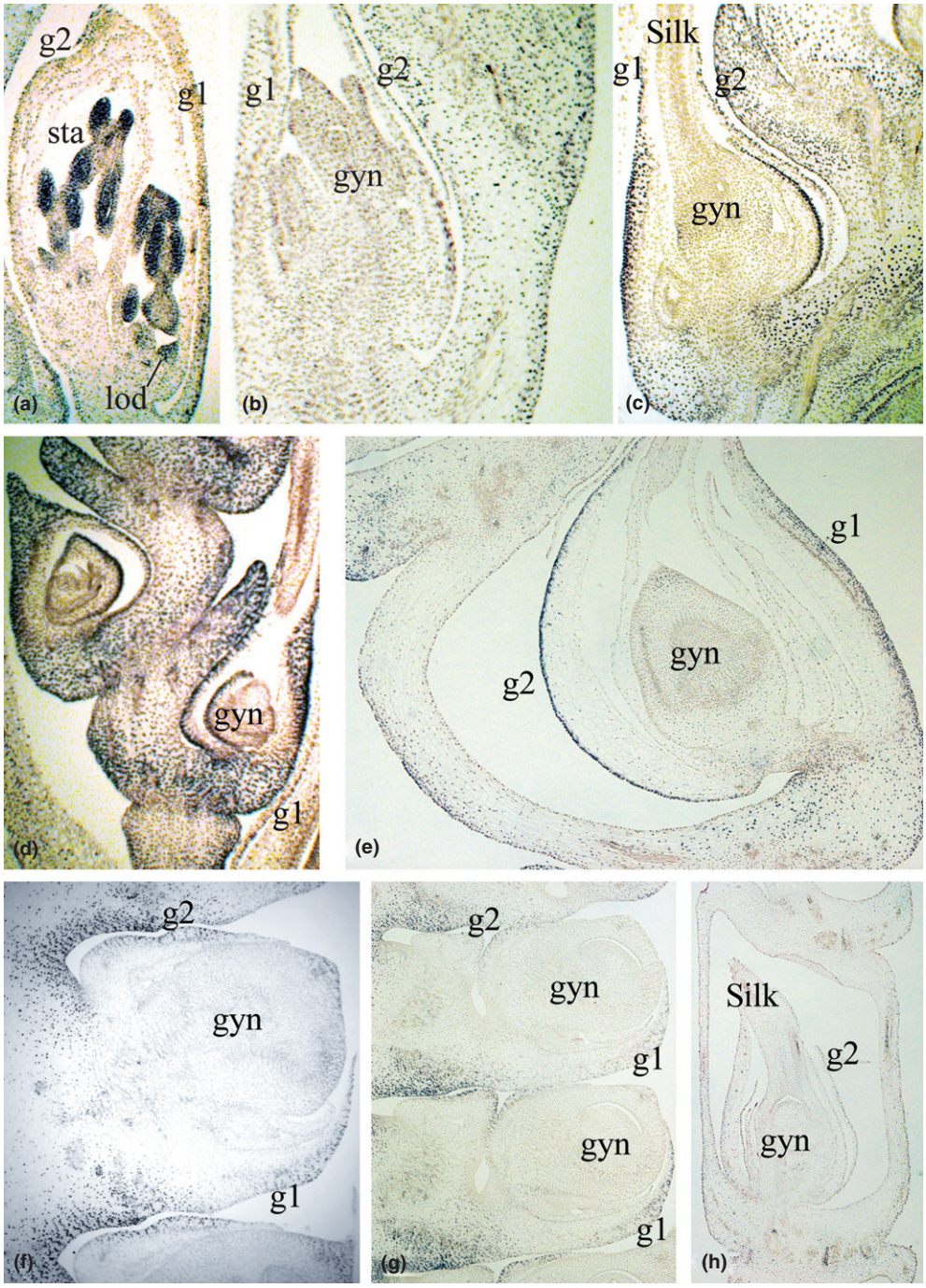

Fig. 4 TGA1-like protein immunolocalization in late-stage spikelet development. (a) In male spikelets of *Tripsacum dactyloides*, TdTGA1 is only expressed in the anthers and lodicules. (b) In silk-stage *T. dactyloides* female spikelets, TdTGA1 is expressed at very low levels, if at all, in glumes, florets and the rachis. (c–e) In silk-stage (c, e) and fruit-stage (d) spikelets of teosinte ears, TGA1/NOT1 is abundantly expressed in the abaxial cells of glumes, is undetectable in the gynoecia and is strongly expressed in the outer epidermal layers of the rachis. (f, g) Silk-stage spikelets of maize ears; TGA1/NOT1 is undetectable in the upper and lower florets, but is moderately to weakly expressed in the abaxial cells of the rachis wall and glumes, respectively. (h) No staining is detectable in teosinte ears in control experiments lacking the TGA1/NOT1 antibody. g1, outer glume; g2, inner glume; gyn, gynoecium.

and late stages of development, TdTGA1 protein expression was barely detectable in the rachis (Figs 3j, 4a,b). In silk-stage ears of maize, TGA1/NOT1 protein was expressed within the wall of the invaginated rachis, but was only weakly detectable in glumes, and was undetectable in gynoecia (Fig. 4f,g). By contrast, although only expressed at low levels in gynoecia, lodicules, paleas and lemmas, TGA1/NOT1 in silk-stage teosinte ears was strongly expressed in the small cells of the abaxial mesophyll of glumes and the rachis (Fig. 4c–e). This pattern of teosinte TGA1/NOT1 expression was maintained following fruit set. No

staining was detectable in control sections lacking the TGA1/NOT1 antibody (Fig. 4h) and the results were consistent between three independent experiments.

tga1/not1 mRNA expression in *Zea*

To determine whether *tga1/not1* expression is distinct from the expression of the corresponding proteins, a single antisense mRNA probe was used to assess the cumulative expression pattern of *tga1/not1* mRNA in maize and teosinte. The expression of *tga1/not1* was similar for maize and teosinte ears at early stages of development (Fig. 5a,d). Before floral differentiation, *tga1/not1* mRNA was detected in the inner and outer glumes, and within the spikelet and floret meristems. At later stages, *tga1/not1* was expressed throughout all floral organ primordia, but was excluded from the expanded region at the base of the outer glume (Fig. 5a,d).

At the silk stage, coincident with thickening of the glumes and rachis invagination in teosinte, *tga1/not1* expression was markedly different between maize and teosinte (Fig. 5b,e,f). In maize, *tga1/not1* was barely detectable in all well-developed spikelet organs and in the invaginated rachis (Fig. 5b). However, in teosinte, *tga1/not1* was abundantly expressed in the large parenchymal cells of the adaxial glume mesophyll and the rachis, but was undetectable in the small cells of the abaxial glume mesophyll (Fig. 5e,f).

In order to differentiate between elevated *tga1* vs *not1* expression in teosinte relative to maize ears, an allele-specific expression assay was carried out (Tables S3, S4). For *tga1*, the average corrected ratio of the teosinte/maize allele expression was 1.06 with a standard deviation of 0.21 (Table S3). Thus, the expression of *tga1* was not significantly different between teosinte and maize ($P = 0.122$). By contrast, for *not1*, the average corrected ratio of the teosinte/maize allele expression was 2.02 with a standard deviation of 1.23 (Table S4). Although the F_1 values varied substantially in allele-specific expression, on average, teosinte *not1* expression was significantly higher than maize *not1* expression ($P = 3.51 \times 10^{-5}$).

Discussion

Several species of Andropogoneae develop hard indigestible structures that surround the growing fruit, potentially allowing them to escape high levels of seed predation and to optimize seed dispersal (Wilkes, 1967). In some species, protection is afforded by a hardened (indurate) lower glume that wraps around the

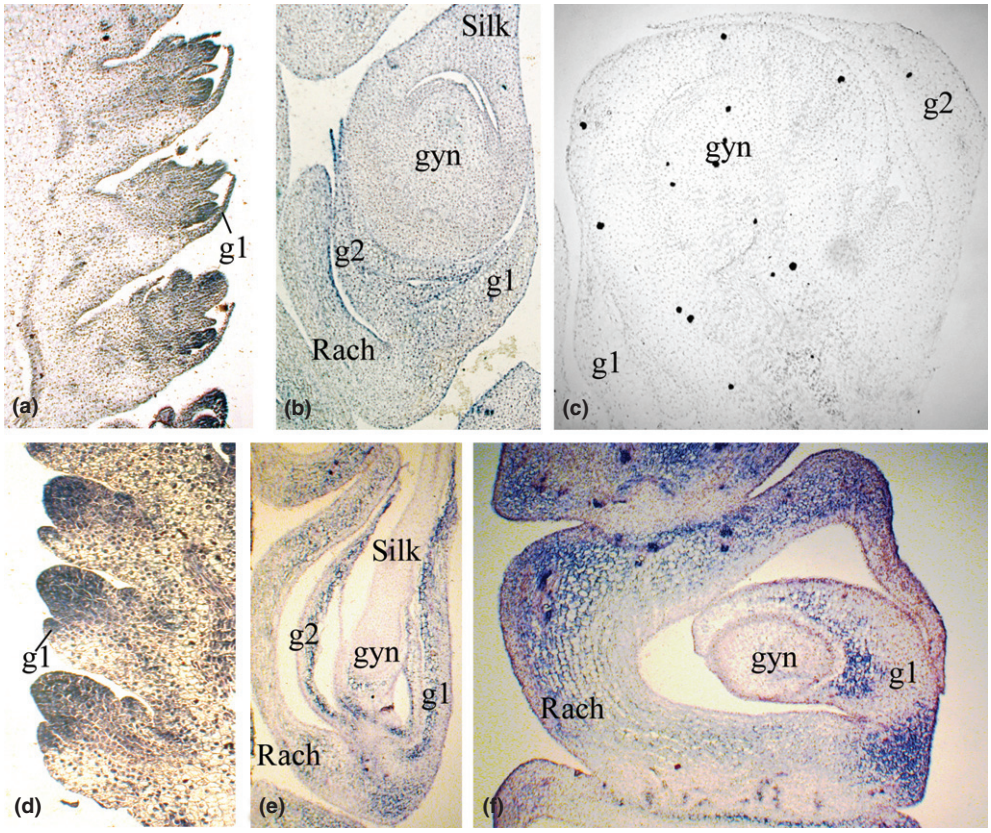

Fig. 5 mRNA *in situ* hybridization of *tga1/not1* in immature and silk-stage ears of maize and teosinte. (a) Immature female spikelets of maize; *tga1/not1* is expressed throughout all organs of the spikelet. (b) Silk-stage spikelet of maize; *tga1/not1* expression is low in glumes and inflorescence axes, and is undetectable in floral organs. (c) Sense control of *tga1/not1* in silk-stage spikelets of maize showing little to no hybridization. (d) Immature female spikelets of teosinte; *tga1/not1* is expressed in glume primordia and in the spikelet meristem. (e) Silk-stage spikelet of teosinte; *tga1/not1* is expressed in the large parenchymal cells of the inflorescence axis and the adaxial side of the inner and outer glumes, but not in the gynoecium. (f) Rachis (Rach) and glumes of teosinte ear; *tga1/not1* is strongly expressed in large, but not small, cells. g1, outer glume; g2, inner glume; gyn, gynoecium.

developing fruit (e.g. *Sorghum*), whereas, in other species, the fruit is shielded by both an indurate glume and a strongly invaginated (sunken) rachis internode (e.g. *Tripsacum*, *Coelorachis* and teosinte) (Clayton & Renvoize, 1986; E. A. Kellogg, pers. obs.). Together with previous studies, our morphological and phylogenetic analyses suggest that indurate glumes have evolved one to three times in the clade containing *Tripsacum* and *Heteropholis*, with at least four secondary transitions back to coriaceous glumes (*Urelytrum*, *P. huillensis*, maize and *Hemarthria* sp.) (Spangler *et al.*, 1999; Lukens & Doebley, 2001; Mathews *et al.*, 2002; Watson & Dallwitz, 1992; Teerawatananon *et al.*, 2011; this study). Similar character reconstructions for invaginated rachis internodes are less apparent. However, they clearly support at least two independent origins of flat to terete internodes, once at the base of *Arundinella* plus Andropogoneae and once at the base of maize, and demonstrate that internode invagination and glume hardness can be uncoupled (Fig. 2).

Evolution and function of *TGA1*-like genes across grasses

Morphological and phylogenetic evidence suggests that hardened glumes and invaginated inflorescence axes have been gained and lost more than once within the Andropogoneae. However, it is unknown whether mutations in orthologous genes are responsible for the independent losses of these traits. In the case of maize, mutations in *tga1* are tightly associated with the evolution of glumes that are membranous, at least apically, and flat inflorescence axes (Dorweiler *et al.*, 1993; Wang *et al.*, 2005). Furthermore, various lines of evidence suggest that the causative mutation underlying the evolution of these traits is within the coding region of *tga1* (Wang *et al.*, 2005). Analysis of the *TGA1*-like gene from multiple species that vary in glume and rachis morphology has revealed a conserved lysine at amino acid position six, as previously found in the *TGA1*-like gene of rice and representative species of *Zea* (except maize) (Wang *et al.*, 2005). Similarly, the microRNA binding site is fully conserved in all *TGA1*-like genes sampled, suggesting purifying selection and conservation of the negative interaction between miR156 (*Cg1*) and *TGA1* (Chuck *et al.*, 2007). Together, these findings suggest that variation in *TGA1*-like amino acid sequences is not correlated with independent losses of hard glumes and invaginated internodes within Andropogoneae. However, as we obtained only partial sequences for many grass species, we cannot rule out the possibility that changes in *TGA1*-like genes have been important for morphological evolution in these species.

An alternative mechanism to explain the reduction in glume hardness and invaginated internodes is evolution at the level of *TGA1*-like gene regulation. This hypothesis predicts differences in protein expression between species that vary in glume and rachis internode morphology. Analyses of protein expression across grasses outside of *Zea* that have membranous to coriaceous glumes (*S. angustifolia*, *A. strigosa*, *E. indica*, *S. viridis*, *C. lacryma-jobi*, pedicellate *S. bicolor* and male *T. dactyloides*), indurate glumes (sessile *S. bicolor* and female *T. dactyloides*), flat or terete rachis internodes (*S. angustifolia*, *A. strigosa*, *E. indica*, *S. viridis* and *C. lacryma-jobi*) and invaginated rachis internodes (*T. dactyloides*) revealed no consistent pattern between morphology and protein expression. Except for maize, this is consistent with functional conservation for TGA1-like proteins across grasses.

The fact that a single amino acid change can simultaneously affect multiple traits suggests that *tga1* is an upstream regulator of the *Z. mays* inflorescence developmental pathway (Wang *et al.*, 2005), and that the development of *Z. mays* glumes and inflorescence axes is tightly coupled. However, the exact function of grass *TGA*-like genes is unclear. Our data show that *TGA1*-like genes have a conserved expression pattern in grass spikelets, being expressed early in spikelet and floral meristems, and at mid-stages of development in glumes and floret organ primordia. Furthermore, in the grass outgroup *J. ascendens*, which has more typical monocot flowers, JaTGA1 is present in all developing floral organs, but is not detectable in the subtending floral bract. Together, these protein expression patterns are similar to the combined expression patterns of *FUL*-like genes, MADS-box transcription factors related to the floral meristem and floral organ identity genes *APETALA1* (*AP1*) and *FUL* of *Arabidopsis thaliana* (Mandel *et al.*, 1992; Mandel & Yanofsky, 1995; Ferrándiz *et al.*, 2000; Preston & Kellogg, 2007; Preston *et al.*, 2009). Indeed, in *A. thaliana* and *Antirrhinum majus*, *tga1* (SPL) homologs directly regulate *FUL*-like genes in leaves and shoot apical meristems (Klein *et al.*, 1996; Wang *et al.*, 2009; Yamaguchi *et al.*, 2009; Preston & Hileman, 2010). Because SPL protein binding site sequences were found in all examined *FUL1* and *FUL2* genes from across the grass family, we posit that the regulatory interaction between SPL and *FUL*-like genes is conserved between core eudicots and grasses. As rice has 19 SPL proteins, most or all of which are expressed in inflorescences (Xie *et al.*, 2006; Yang *et al.*, 2008), future analyses of *FUL*-like gene expression in *tga1*-like silenced lines will be required to specifically test the hypothesis of TGA1–*FUL* interaction.

TGA1 and domestication of the maize ear

Probably the most striking example of glume and rachis evolution is between the ears of maize and its ancestor teosinte. Although teosinte has indurate glumes and strongly invaginated inflorescence axes, reduced hardness and flat axes have been selected for in maize glumes. Previous studies have revealed an important role for *tga1* in the domestication of maize (Dorweiler *et al.*, 1993; Wang *et al.*, 2005). These morphological differences were associated with six fixed differences in the promoter and one amino acid difference in the protein-coding region of the SPL gene *tga1* (Wang *et al.*, 2005).

Several lines of evidence suggest that the amino acid difference in *tga1* underlies the inflorescence differences between maize and teosinte. First, the lysine of teosinte in this position has been conserved through grass evolution, including taxa as disparate as rice (Ehrhartoideae), wheat (Pooideae) and *R. aurita* (Panicoideae) (Wang *et al.*, 2005; this study). Indeed, extensive sequencing from multiple teosinte populations found this to be the only fixed difference between maize and teosinte; the six promoter polymorphisms are variable within teosinte (Zhao, 2006). Second, a

single nonconservative mutation in an amino acid adjacent to the potentially causative amino acid of maize *tga1* results in teosinte-like glume and rachis internode structures (Wang *et al.*, 2005). Finally, the identification of a *tga1* paralog (*not1*) explains the apparent differences between the *tga1* gene and TGA1 protein expression patterns in maize and teosinte reported in Wang *et al.* (2005). Specifically, quantitative (q)RT-PCR analyses previously showed no difference in *tga1* RNA levels between early- to silk-stage maize and teosinte ears (Wang *et al.*, 2005). By contrast, we found a quantitative difference in RNA levels between maize and teosinte lower glumes and rachis internodes by *in situ* hybridization (Wang *et al.*, 2005). Protein levels were also different between the two, as measured by western blots and immunolocalization (Wang *et al.*, 2005). The qRT-PCR primers are specific to *tga1* alone, and therefore we conclude that gene expression is indeed similar between maize and teosinte. However, the *in situ* probe and antibody probably capture both *tga1*/TGA1 and *not1*/NOT1 expression, so that elevated RNA and protein levels in late-stage teosinte ears reflect higher expression of *not1*/NOT1 rather than *tga1*/TGA1. This interpretation is strongly supported by our allele-specific expression data. We infer that the expression of the *tga1* gene and its protein product are thus quantitatively similar between the two species. Therefore, our data do not support the hypothesis that differences in the teosinte and maize glume and rachis are a result of variation in protein stability or translational efficiency. Instead, we prefer the hypothesis that the replacement of either residue five or six of TGA1 changes its biochemical function and causes the glume and rachis differences between maize and teosinte.

Acknowledgements

We thank Sherry Flint-Garcia for providing flowering material of teosinte, and Shelby Kleweis, Jimena Nores and Chris Gillespie for help with sequencing. This research was funded by the National Science Foundation grants DBI-0820619 (J.D.) and DBI-0110189 (E.A.K.).

References

Birkenbihl RP, Jach G, Saedler H, Huijser P. 2005. Functional dissection of the plant-specific SBP-domain: overlap of the DNA-binding and nuclear localization domains. *Journal of Molecular Biology* **352**: 585–596.

Bomblies K, Doebley JF. 2005. Molecular evolution of *FLORICAULA/ LEAFY* orthologs in the Andropogoneae (Poaceae). *Molecular Biology and Evolution* **22**: 1082–1094.

Celarier R. 1956. Cytotaxonomy of the Andropogoneae. I. Subtribes Dimeriinae and Saccharinae. *Cytologia* **21**: 272–291.

Cheng PC, Greyson RI, Walden DB. 1983. Organ initiation and the development of unisexual flowers in the tassel and ear of *Zea mays*. *American Journal of Botany* **70**: 450–462.

Chuck G, Cigan M, Saeteurn K, Hake S. 2007. The heterochronic maize mutant Corngrass1 results from overexpression of a tandem microRNA. *Nature Genetics* **39**: 544–549.

Clayton WD, Renvoize SA. 1986. *Genera* graminum. London, UK: Her Majesty's Stationery Office.

Clifford HT. 1987. Spikelet and floral morphology. In: Soderstrom TR, Hilu K, Campbell CS, Barkworth ME, eds. *Grass systematics and evolution*. Washington, DC, USA: Smithsonian Institute Press, 21–30.

Dorweiler J, Doebley J. 1997. Developmental analysis of *teosinte glume architecture1*: a key locus in the evolution of maize (Poaceae). *American Journal of Botany* **84**: 1313–1322.

Dorweiler J, Stec A, Kermicle J, Doebley J. 1993. *Teosinte glume architecture1*: a genetic locus controlling a key step in maize evolution. *Science* **262**: 233–235.

Ewing B, Hillier L, Wendl MC, Green P. 1998. Base-calling of automated sequencer traces using phred. I. Accuracy assessment. *Genome Research* **8**: 175–185.

Ferrándiz C, Gu Q, Martienssen R, Yanofsky MF. 2000. Redundant regulation of meristem identity and plant architecture by *FRUITFULL*, *APETALA1* and *CAULIFLOWER*. *Development* **12**: 725–734.

Grass Phylogeny Working Group. 2001. Phylogeny and subfamilial classification of the grasses (Poaceae). *Annals of the Missouri Botanical Garden* **88**: 373–457.

Ikeda K, Sunohara H, Nagato Y. 2004. Developmental course of inflorescence and spikelet in rice. *Breeding Science* **54**: 147–156.

Jackson D. 1991. *In situ* hybridization in plants. In: Bowles DJ, Gurr SJ, McPherson M, eds. *Molecular plant pathology: a practical approach*. Oxford, UK: Oxford University Press, 163–174.

Jackson D, Veit B, Hake S. 1994. Expression of maize *KNOTTED1* related homeobox genes in the shoot apical meristem predicts patterns of morphogenesis in the vegetative shoot. *Development* **120**: 405–413.

Jiao Y, Wang Y, Xue D, Wang J, Yan M, Liu G, Dong G, Zeng D, Lu Z, Zhu X *et al.* 2010. Regulation of *OsSPL14* by OsmiR156 defines ideal plant architecture in rice. *Nature Genetics* **42**: 541–545.

Klein J, Saedler H, Huijser P. 1996. A new family of DNA binding proteins includes putative transcriptional regulators of the *Antirrhinum majus* floral meristem identity gene *SQUAMOSA*. *Molecular and General Genetics* **250**: 7–16.

Liang X, Nazarenus TJ, Stone JM. 2008. Identification of a consensus DNA-binding site for the *Arabidopsis thaliana* SBP domain transcription factor, *AtSPL14*, and binding site kinetics by surface plasmon resonance. *Biochemistry* **47**: 3645–3653.

Lucas WJ, Boche-Pillon S, Jackson DP, Nguyen L, Baker L, Ding B, Hake S. 1995. Selective trafficking of KNOTTED1 homeodomain protein and its mRNA through plasmadesmata. *Science* **270**: 1980–1983.

Lukens L, Doebley J. 2001. Molecular evolution of the *teosinte branched* gene among maize and related grasses. *Molecular Biology and Evolution* **18**: 627–638.

Maddison DR, Maddison WP. 2003. *MacClade: analysis of phylogeny and character evolution*. Sunderland, MA, USA: Sinauer Associates.

Maddison DR, Maddison WP. 2006. *StochChar: a package of Mesquite modules for stochastic models of character evolution, version 1.1*. [WWW document]. URL http://mesquiteproject.org. [accessed on 21 June 2008].

Maddison DR, Maddison WP. 2007. *Mesquite: a modular system for evolutionary analysis, version 2.01*. [WWW document]. URL http://mesquiteproject.org. [accessed on 21 June 2008].

Malcomber ST, Kellogg EA. 2004. Heterogeneous expression patterns and separate role of the *SEPALLATA* gene *LEAFY HULL STERILE1* in grasses. *Plant Cell* **16**: 1692–1706.

Malcomber ST, Kellogg EA. 2006. Evolution of unisexual flowers in grasses (Poaceae) and the putative sex-determination gene, *TASSELSEED2* (*TS2*). *New Phytologist* **170**: 885–899.

Mandel MA, Gustafson-Brown C, Savidge B, Yanofsky MF. 1992. Molecular characterization of the *Arabidopsis* floral homeotic gene *APETALA1*. *Nature* **360**: 273–277.

Mandel MA, Yanofsky MF. 1995. The *Arabidopsis AGL8* MADS box gene is expressed in inflorescence meristems and is negatively regulated by *APETALA1*. *Plant Cell* **7**: 1763–1771.

Manning K, Tör M, Poole M, Hong Y, Thompson AJ, King GJ, Giovannoni JJ, Seymour GB. 2006. A naturally occurring epigenetic mutation in a gene encoding an SBP-box transcription factor inhibits tomato fruit ripening. *Nature Genetics* **38**: 948–952.

Mathews S, Spangler RE, Mason-Gamer RJ, Kellogg EA. 2002. Phylogeny of Andropogoneae inferred from phytochrome B, GBSSI, and *ndhF*. *International Journal of Plant Science* **163**: 441–450.

Nylander JAA. 2004. *MrModeltest v2*. (program distributed by the author). Uppsala, Sweden: Evolutionary Biology Centre, Uppsala University.

Preston JC, Christensen A, Malcomber ST, Kellogg EA. 2009. MADS-box gene expression and implications for developmental origins of the grass spikelet. *American Journal of Botany* **96**: 1419–1429.

Preston JC, Hileman LC. 2010. SQUAMOSA-PROMOTER BINDING PROTEIN 1 initiates flowering in *Antirrhinum majus* through the activation of meristem identity genes. *The Plant Journal* **62**: 704–712.

Preston JC, Kellogg EA. 2006. Reconstructing the evolutionary history of paralogous *APETALA1/ FRUITFULL*-like genes in grasses (Poaceae). *Genetics* **174**: 421–437.

Preston JC, Kellogg EA. 2007. Conservation and divergence of *APETALA1/ FRUITFULL*-like gene function in grasses: evidence from gene expression analyses. *Plant Journal* **52**: 69–81.

Ronquist F, Huelsenbeck JP. 2003. MrBayes 3: Bayesian phylogenetic inference under mixed models. *Bioinformatics* **19**: 1572–1574.

Sánchez-Ken JG, Clark LG, Kellogg EA, Kay EA. 2007. Reinstatement and emendation of subfamily Micrairoideae (Poaceae). *Systematic Botany* **32**: 71–80.

Schwarz S, Grande AV, Bujdoso N, Saedler H, Huijser P. 2008. The microRNA regulated SBP-box genes *SPL9* and *SPL15* control shoot maturation in *Arabidopsis*. *Plant Molecular Biology* **67**: 183–195.

Spangler R, Zaitchik B, Russo E, Kellogg E. 1999. Andropogoneae evolution and generic limits in *Sorghum* (Poaceae) using *ndhF* sequences. *Systematic Botany* **24**: 267–281.

Teerawatananon A, Jacobs SWL, Hodkinson TR. 2011. Phylogenetics of *Panicoideae* (Poaceae) based on chloroplast and nuclear DNA sequences. *Telopea* **13**: 115–142.

Wang H, Nussbaum-Wagler T, Li B, Zhao Q, Vigouroux Y, Faller M, Bomblies-Yant K, Lukens L, Doebley J. 2005. The origins of naked grains of maize. *Nature* **436**: 714–719.

Wang JW, Czech B, Weigel D. 2009. miR156-regulated SPL transcription factors define an endogenous flowering pathway in *Arabidopsis thaliana*. *Cell* **138**: 738–749.

Watson L, Dallwitz MJ. 1992. *The grass genera of the world*. Wallingford, UK: CAB International.

Wilkes HG. 1967. *Teosinte: the closest relative of maize*. Cambridge, MA, USA: Bussey Institution of Harvard University.

Xie K, Wu C, Xiong L. 2006. Genomic organization, differential expression, and interaction of SQUAMOSA promoter-binding-like transcription factors and microRNA156 in rice. *Plant Physiology* **142**: 280–293.

Yamaguchi A, Wu MF, Yang L, Wu G, Poethig S, Wagner D. 2009. The microRNA-regulated SBP-box transcription factor SPL3 is a direct upstream activator of *LEAFY*, *FRUITFULL*, and *APETALA1*. *Developmental Cell* **17**: 268–278.

Yang Z, Wang X, Gu S, Hu Z, Xu H, Xu C. 2008. Comparative study of SBP-box gene family in *Arabidopsis thaliana* and rice. *Gene* **407**: 1–11.

Zhao Q. 2006. *Molecular population genetics of maize regulatory genes during maize evolution*. PhD dissertation, University of Wisconsin, Madison, WI, USA.

Zwickl DJ. 2006. *Genetic algorithm approaches for the phylogenetic analysis of large biological sequence data sets under the maximum likelihood criterion*. PhD dissertation, University of Texas at Austin, Austin, TX, USA.

Supporting Information

Additional supporting information may be found in the online version of this article.

Fig. S1 Phylogenetic relationships of grass *FUL*-like genes and number of associated SPL binding sequences in the putative promoters and introns.

Fig. S2 Andropogoneae species relationships based on combined analyses of *waxy*, *ndhF*, *phyB*, *tb1* and *tga1*-like genes.

Table S1 Species sampled for phylogenetic analyses of *tga1* with vouchers and GenBank accession numbers.

Table S2 Species sampled for combined phylogenetic analyses with vouchers and GenBank accession numbers.

Table S3 *tga1* allele-specific expression assay.

Table S4 *not1* allele-specific expression assay.

Please note: Wiley-Blackwell are not responsible for the content or functionality of any supporting information supplied by the authors. Any queries (other than missing material) should be directed to the *New Phytologist* Central Office.